ELSEVIER

Human Movement Science 19 (2000) 425–449

HUMAN MOVEMENT SCIENCE

www.elsevier.com/locate/humov

The HKB model revisited: How varying the degree of symmetry controls dynamics

Armin Fuchs *, Viktor K. Jirsa

Center for Complex Systems and Brain Sciences, Florida Atlantic University, 777 Glades Road, Boca Raton, FL 33431, USA

Abstract

In human bimanual coordination an in-phase movement pattern is typically preferred to an anti-phase pattern. This preference results from a symmetry breaking in the dynamics between its components whose degree can be altered not only by variation of environmental but also intrinsic constraints. Recently, Carson et al. [Experimental Brain Research, 131, 196–214 (2000)] operationalized this notion and induced phase transitions from in-phase to anti-phase movement patterns. Here, we tackle this situation theoretically by introducing an additional parameter which represents the degree of symmetry into the HKB equation of bimanual coordination. We predict new phenomena to be observed experimentally when this parameter is manipulated independently or together with the movement rate. We derive the statistical properties of the extended system from a stochastic theory in detail and suggest how the predicted phenomena can be tested experimentally.

PsycINFO classification: 2240; 2260

Keywords: Bimanual; Symmetry; Motor; Coordination; Oscillator; Dynamics

* Corresponding author. Tel.: +1-561-297-0125; fax: +1-561-297-3634.
E-mail address: fuchs@walt.ccs.fau.edu (A. Fuchs).

0167-9457/00/$ - see front matter
PII: S0167-9457(00)00025-7

1. Introduction

Transition phenomena observed in the coordinated movements of human limbs have been investigated systematically for more than 15 years in a variety of experimental paradigms and manipulations. These studies include bimanual finger coordination in a symmetric and anti-symmetric fashion (Kelso, 1984; Haken, Kelso & Bunz, 1985), syncopation and synchronization of single limb movement with a metronome (Kelso, DelColle & Schöner, 1990), coordination of different limbs, for example an arm and a leg (Kelso & Jeka, 1992) including manipulations of the mechanical properties of the components involved, and even between two subjects coordinating their leg movements while watching each other (Schmidt, Carello & Turvey, 1990). At slow movement rates two stable coordination patterns are found which can be classified as in-phase (defined as homologous muscle groups being activated simultaneously) and anti-phase (if these muscles are activated in an alternating fashion). In most cases, with an increase of the cycling frequency an initial anti-phase pattern becomes unstable and subjects switch spontaneously to the in-phase mode. If a movement is started in-phase no transitions are observed for an increase or for a decrease in the cycling frequency. Haken et al. (1985) modeled this behavior on a phenomenological level as a switch in the relative phase between the two limbs and derived an equation of motion from coupled nonlinear oscillators representing the single limbs. The specific form of the coupling function used led to a dynamical system that is bistable for certain values of a control parameter (the movement frequency) and becomes monostable when this parameter exceeds a certain threshold.

Recently, Carson, Rick, Smethurst, Lison and Byblow (2000) showed that bimanual pronation [1] (an, in-phase movement with respect to the above definition) becomes unstable at a certain cycling frequency if on one side the axis of rotation is located above and on the other side below the hand (see Fig. 1). The situation is similar for bimanual supination in the same setup, and both, initial bimanual pronation and the other supinating (an anti-phase pattern) at the end of the trials. When the two axes are at the same location with respect to the hands the former patterns are stable and pronating with

[1] Here pronation (supination) means to reach peak pronation (supination) at the beat of the metronome and the opposite peak while the metronome was silent. In all cases these were full pronation–supination movements.

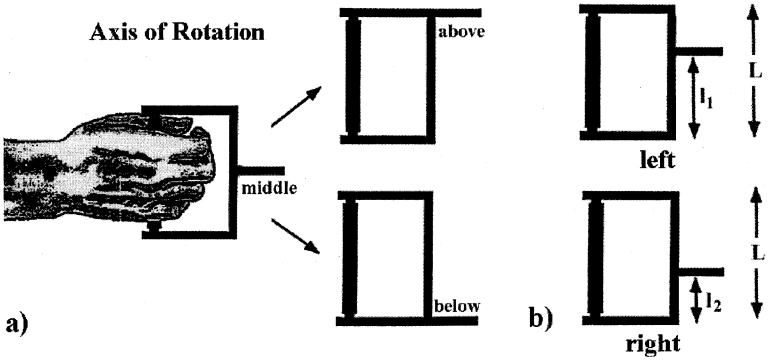

Fig. 1. Manipulating the axes of rotation: (a) The manipulandum used by Carson et al. is shown which allows pronation and supination movements around an axis in the middle, above or below the hand. (b) Location of the axes for the left and right hand can be changed continuously leading to a new control parameter σ.

one hand, supinating with the other becomes unstable at sufficiently high movement rates.

The HKB model in its original form describes a switch from anti-phase to in-phase coordination when a control parameter, related to the movement frequency, exceeds a certain threshold. However, here both end effectors are assumed to be identical and the axes of rotation are located symmetrically in agreement with Carson's recent results. No switching occurs when the coordination is initially in-phase. With the manipulation of the axes in the Carson et al. experiment, transitions from in-phase to anti-phase were found which cannot be accounted for in the original HKB model.

Carson et al.'s experiment and its results provide an entry point to the theoretical understanding of the degree of symmetry breaking in the dynamics of a complex system. In the theoretical description so far the anti-phase and in-phase movement patterns are equivalent behavioral states, distinguished only by the preference of the in-phase state at high movement frequencies. This preference results from a symmetry breaking in the dynamics (i.e. the coupling) of the components commonly understood to be central nervous (see Jirsa, Fuchs & Kelso, 1998) where a neural basis for the HKB coupling is provided). However, also environmental and/or intrinsic constraints may alter the degree of symmetry breaking which we quantify as a scalar quantity, the symmetry parameter σ. In the Carson et al. experiment this parameter must be related to the positions of the axes of rotation for the single limbs and can be varied continuously.

Here, we present an extension of the HKB model which describes all cases studied in the experiment but also predicts behavior that should be observed with axes located not only above and below the hands (the extreme cases studied by Carson et al.) but also somewhere in between. Based on symmetry properties we derive additional terms for the coupling between two oscillators in a way that transitions from in-phase to anti-phase can be modeled. Moreover, we will predict the phenomena that should be found for arbitrary locations of the axes of rotation and discuss the stability of the movement patterns in detail.

The paper is organized as follows: Section 2 summarizes the experimental setup and the results of the Carson et al. experiment as far as they are relevant here. In Section 3 we derive the equation of motion for the relative phase which contains the extension needed to model the findings and make the predictions mentioned above from the level of coupled nonlinear oscillators. In Section 4 we discuss how the predictions can be tested experimentally in a qualitative and quantitative fashion and Section 5 contains assumptions and procedures needed to connect theory and experiment quantitatively. In Section 6 we summarize and discuss the theoretical results.

2. Experimental findings

In a series of experiments Carson et al. (2000) studied the stability of unimanual and bimanual pronation and supination movement patterns under a manipulation of the cycling frequency and of the locations of the axes of rotation. In the bimanual case an apparatus was used that fixed the axes of rotation in the middle, above or below the hand as shown in Fig. 1(a).

Subjects were instructed to perform one out of four movement conditions paced by a metronome starting at a frequency of 1.25 Hz and increasing by 0.25 Hz every 8 s up to 3 Hz. The four conditions were classified as in-phase (both limbs pronating simultaneously or supinating simultaneously) and anti-phase (left/right limb pronating and the other supinating). Stable movement patterns throughout the trials were found for the in-phase initial condition if both axes of rotation were either above or below the hand, and initial anti-phase was stable if the axes of rotation for the two hands were different. Spontaneous transitions from anti-phase to in-phase with increasing movement frequency were found with the axes located both on top or bottom and from in-phase to anti-phase when the movement was performed around different axes. Fig. 2 shows representative trials for two of the four

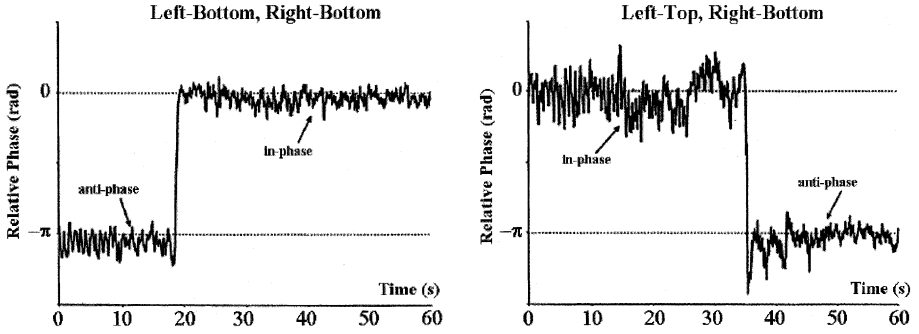

Fig. 2. Time series of the relative phase from two representative trials showing the switch from anti-phase to in-phase (left) and vice versa (right) under manipulation of the axes of rotation for the two hands (compare text).

conditions. The most striking aspect of this experiment is the change in the stability of the movement patterns depending on whether the axes of rotations are on the same or on opposite sides of the hands and, more important here, the possibility to manipulate the axes locations in an experiment in a continuous way as indicated in Fig. 1(b).

3. Extending the HKB theory

The HKB model, originally introduced to describe spontaneous transitions observed in coordinated bimanual finger or hand movements, identifies the relative phase, ϕ, as the order-parameter whose dynamics is captured by an equation of motion of the form

$$\dot{\phi} = -a \sin \phi - 2b \sin 2\phi. \tag{1}$$

The dynamical properties of this equation are well known and can be summarized as follows:

- For all values of $a > 0$ and $b > 0$ there are fixed points $\phi_0 = 0$ and $\phi_\pi = \pi$ corresponding to in-phase and anti-phase movement, respectively.
- In the parameter region $b/a > 1/4$ corresponding to low cycling frequencies for the limbs both fixed points are stable, i.e., movements can be performed either in the in-phase or in the anti-phase coordination mode.
- In the parameter region $b/a < 1/4$, i.e., for high cycling frequencies the fixed point ϕ_π is unstable and the only remaining stable fixed point is ϕ_0 corresponding to an in-phase movement pattern.

It is our goal to extend (1) such that transitions in both directions can be modeled, i.e., from anti-phase to in-phase but also from in-phase to anti-phase as observed in the Carson et al. experiment. To this end we will derive additional terms in the coupling function for the oscillators representing the single limbs such that there is a symmetry between in-phase and anti-phase coordination. Eq. (1) does not have this property (for $a, b > 0$) and predicts that the in-phase mode is stable for all movement frequencies whereas the anti-phase pattern can not be executed at high movement rates. We will perform three steps to find an equation of motion for the dynamics of relative phase with an additional parameter which allows for tuning the stability of the in-phase and anti-phase mode in a continuous fashion. Starting from standard equations for coupled oscillators with $x_k(t)$ and their derivatives representing the finger locations, velocities and accelerations we employ a coordinate transformation originally developed in Jirsa et al. (1998) which shows the asymmetry between the coordination patterns more explicitly. We add a term such that the equations become symmetric and apply the inverse transformation leading us back to the original representation with additional terms in the coupling function. Then, following the lines of HKB (Haken et al., 1985), we split $x_k(t)$ into amplitude and phase in order to obtain an equation for the dynamics of relative phase. For these calculations we use the so-called hybrid oscillator which has been shown to approximate certain properties of human limb movement (Kay, Kelso, Saltzman and Schöner, 1987). However, the final equation for the relative phase does not depend on the specific form used for the oscillators.

Bimanual coordination can be described by two-coupled hybrid oscillators for the left and right limb of the form:

$$\begin{aligned} \ddot{x}_1 + \epsilon\dot{x}_1 + \omega^2 x_1 + \gamma x_1^2\dot{x}_1 + \delta\dot{x}_1^3 &= (\dot{x}_1 - \dot{x}_2)\{\alpha + \beta(x_1 - x_2)^2\}, \\ \ddot{x}_2 + \epsilon\dot{x}_2 + \omega^2 x_2 + \gamma x_2^2\dot{x}_2 + \delta\dot{x}_2^3 &= (\dot{x}_2 - \dot{x}_1)\{\alpha + \beta(x_2 - x_1)^2\}. \end{aligned} \tag{2}$$

The left-hand side of (2) shows self-sustained oscillation for the linear damping constant $\epsilon < 0$ and the parameters of the nonlinearities (the Rayleigh and the van der Pol term) $\gamma, \delta > 0$. The right-hand side is the HKB coupling which is known to lead to a dynamical equation for the relative phase of the form (1).

The system (2) can be split into symmetric and anti-symmetric coordinates ψ_+ and ψ_- defined as

$$\psi_+ = x_1 + x_2 \quad \text{and} \quad \psi_- = x_1 - x_2, \tag{3}$$

where ψ_+ vanishes for an anti-phase movement and $\psi_- = 0$ for an in-phase movement (see, e.g., Jirsa et al., 1998, 1999 for details). The dynamics in these new coordinates is found by substituting the inverse of (3),

$$x_1 = \frac{1}{2}(\psi_+ + \psi_-) \quad \text{and} \quad x_2 = \frac{1}{2}(\psi_+ + -\psi_-), \tag{4}$$

into the original Eq. (2) and reads

$$\begin{aligned}
&\ddot{\psi}_+ + \epsilon\dot{\psi}_+ + \omega^2\psi_+ + \frac{\gamma}{12}\frac{\mathrm{d}}{\mathrm{d}t}(\psi_+^3 + 3\psi_-^2\psi_+) + \frac{\delta}{4}(\dot{\psi}_+^3 + 3\dot{\psi}_-^2\dot{\psi}_+) = 0,\\
&\ddot{\psi}_- + \epsilon\dot{\psi}_- + \omega^2\psi_- + \frac{\gamma}{12}\frac{\mathrm{d}}{\mathrm{d}t}(\psi_-^3 + 3\psi_+^2\psi_-) + \frac{\delta}{4}(\dot{\psi}_-^3 + 3\dot{\psi}_+^2\dot{\psi}_-) = 2\dot{\psi}_-(\alpha + \beta\psi_-^2).
\end{aligned} \tag{5}$$

The system (2) is invariant under an exchange of x_1 and x_2, i.e., exchanging the role of the two limbs. The system (5) is not invariant under exchange of the quantities ψ_+ and ψ_- because the right-hand side of the first equation vanishes, i.e., it is independent of the coupling parameters α and β. The coupling appears only in the second equation and only depends on ψ_-, the anti-phase mode, and not on the in-phase mode ψ_+. Because of this asymmetry the systems (2) and (5) exhibit only transitions from anti-phase to in-phase but not vice versa. In the Carson et al. experiment this corresponds to a situation where the location of the axes of rotation is the same for both limbs. Now we introduce a symmetry parameter σ into (5) such that for $\sigma = 0$ we obtain the system (5) where the anti-phase movement becomes unstable at a critical frequency ω_c. For $\sigma = 1$ we require the opposite behavior, i.e., in-phase movement becomes unstable and for high movement rates the only stable coordination mode is anti-phase which corresponds to a situation with the axis above the hand on one side and below the hand on the other side. This scenario appears to be fully equivalent to the former ($\sigma = 0$) with the roles of in-phase an anti-phase exchanged. The extended system is given by

$$\begin{aligned}
&\ddot{\psi}_+ + \epsilon\dot{\psi}_+ + \omega^2\psi_+ + \frac{\gamma}{12}\frac{\mathrm{d}}{\mathrm{d}t}(\psi_+^3 + 3\psi_-^2\psi_+) + \frac{\delta}{4}(\dot{\psi}_+^3 + 3\dot{\psi}_-^2\dot{\psi}_+)\\
&\quad = 2\sigma\dot{\psi}_+(\alpha + \beta\psi_+^2),\\
&\ddot{\psi}_- + \epsilon\dot{\psi}_- + \omega^2\psi_- + \frac{\gamma}{12}\frac{\mathrm{d}}{\mathrm{d}t}(\psi_-^3 + 3\psi_+^2\psi_-) + \frac{\delta}{4}(\dot{\psi}_-^3 + 3\dot{\psi}_+^2\dot{\psi}_-)\\
&\quad = 2(1-\sigma)\dot{\psi}_-(\alpha + \beta\psi_-^2).
\end{aligned} \tag{6}$$

Notice that for $\sigma = 1$ (6) has the same structure as (5) with the roles of ψ_+ and ψ_- reversed. We now go back to a representation in the original variables x_1 and x_2 by adding and subtracting the two equations in (6), respectively:

$$\begin{aligned}
\ddot{x}_1 + \cdots &= \frac{1}{2}(\ddot{\psi}_+ + \ddot{\psi}_-) + \cdots = \dot{\psi}_-(\alpha + \beta\psi_-^2) + \sigma\{\dot{\psi}_+(\alpha + \beta\psi_+^2) - \dot{\psi}_-(\alpha + \beta\psi_-^2)\}, \\
\ddot{x}_2 + \cdots &= \frac{1}{2}(\ddot{\psi}_+ - \ddot{\psi}_-) + \cdots = -\dot{\psi}_-(\alpha + \beta\psi_-^2) + \sigma\{\dot{\psi}_+(\alpha + \beta\psi_+^2) + \dot{\psi}_-(\alpha + \beta\psi_-^2)\}.
\end{aligned} \tag{7}$$

As we only changed the coupling on the right-hand side the oscillators on the left-hand side are still the same as in (2) and we rewrite them only in the symbolic way $\ddot{x}_{1,2} + \cdots$. In fact, our resulting equations must be invariant under the exchange of x_1 and x_2 and it is therefore sufficient to calculate only one of them, say $\ddot{x}_1$.

Resubstituting (3) into the left-hand side of (7) we obtain after straightforward calculations

$$\begin{aligned}
\ddot{x}_1 + \cdots &= (\dot{x}_1 - \dot{x}_2)\{\alpha + \beta(x_1 - x_2)^2\} + 2\sigma\{\alpha\dot{x}_2 + \beta[\dot{x}_2 x_1^2 + \dot{x}_2 x_2^2 + 2\dot{x}_1 x_1 x_2]\}, \\
\ddot{x}_2 + \cdots &= (\dot{x}_2 - \dot{x}_1)\{\alpha + \beta(x_2 - x_1)^2\} + 2\sigma\{\alpha\dot{x}_1 + \beta[\dot{x}_1 x_2^2 + \dot{x}_1 x_1^2 + 2\dot{x}_2 x_2 x_1]\}.
\end{aligned} \tag{8}$$

The first term on the right-hand side in both equations of (8) is identical to the HKB coupling in the original system (2) and independent of the symmetry parameter σ. The second term, which vanishes for $\sigma = 0$, originates from the extensions introduced into (6) and its specific form is certainly not trivial. However, for $\sigma = 1$ this system undergoes a transition from in-phase to anti-phase and not vice versa as shown by the numerical simulations in Fig. 3.

The next step is to derive an equation for the dynamics of relative phase analogous to the original HKB equation. To this end we split x_k into an amplitude r (which we treat as a constant and assume to be the same for $k = 1, 2$) and a phase $\varphi_k(t)$, and derive the equation of motion for the relative phase $\phi = \varphi_1 - \varphi_2$. These calculations are given explicitly in Appendix A and lead to

$$\dot{\phi} = -(1 - 2\sigma)a \sin\phi - 2b \sin 2\phi. \tag{9}$$

As in the original HKB model the equation of motion can be derived from a potential function

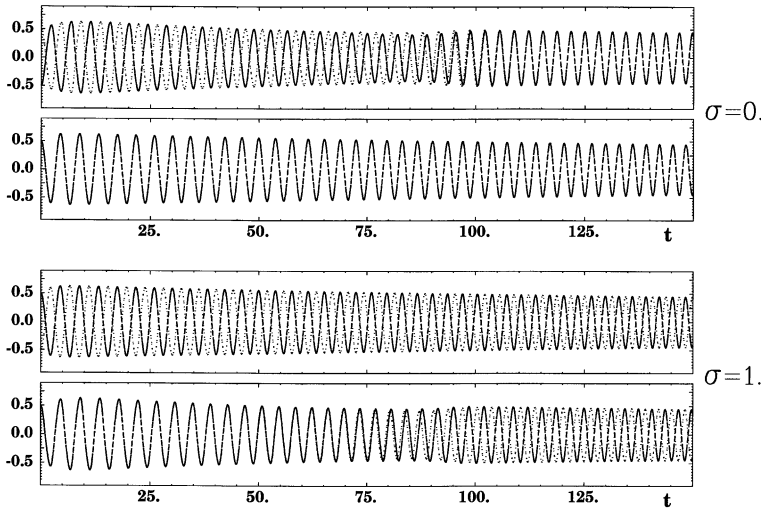

Fig. 3. Numerical simulations of (8) for the cases $\sigma = 0$ (top two plots) and $\sigma = 1$ (bottom two plots) with initial conditions in anti-phase and in-phase. The frequency is continuously increased from $\omega = 1.4$ on the left to $\omega = 2.1$ on the right. The anti-phase (in-phase) condition is stable for $\sigma = 1$ ($\sigma = 0$) and switching occurs from anti-phase to in-phase for $\sigma = 0$ and from in-phase to anti-phase for $\sigma = 1$. Other parameters used: $\epsilon = -0.7, \gamma = \delta = 1, \alpha = -0.2, \beta = 0.5$.

$$\dot{\phi} = -\frac{\partial V(\phi)}{\partial \phi} \quad \text{with } V(\phi) = -(1 - 2\sigma)a\cos\phi - b\cos 2\phi. \tag{10}$$

Fig. 4 shows plots of the potential landscape for different values of $k = b/a$ and σ. It is evident that the role of in-phase and anti-phase behavior in the first ($\sigma = 0$) and last ($\sigma = 1$) column are exchanged. Obviously, $\sigma = 0$ represents the original HKB case and in the Carson et al. experiment the situation where the axes are on the same side of the hands. For values of $k > 0.25$ corresponding to low movement rates of fixed points $\phi_0 = 0$ and $\phi_\pi = \pi$ are stable. As k decreases (which corresponds to an increase in the cycling frequency) and exceeds its critical value, ϕ_π loses its stability and the only stable fixed point remaining is ϕ_0, i.e., in-phase movement. The opposite is true for $\sigma = 1$, the situation where the axes are located on opposite sides. The minimum of the potential for the fixed point ϕ_0 is not as deep as the minimum at ϕ_π at slow movement rates. As the movement speeds up the in-phase minimum becomes a maximum and any initial in-phase movement will undergo a switch to anti-phase.

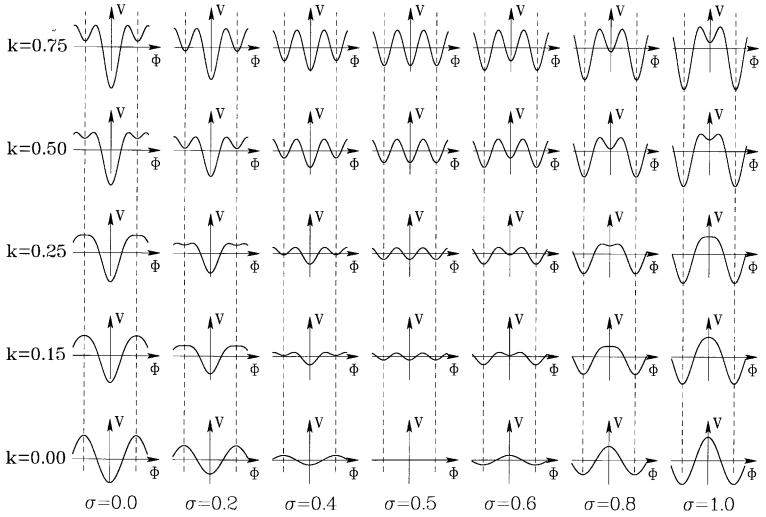

Fig. 4. Potential functions for relative phases ϕ from (10) for different values of $k = b/a$ and σ. The vertical dashed lines correspond to $\phi = \pm\pi$.

In summary, the extended version (9) of the HKB equation derived above describes the experimentally observed phenomena qualitatively. The predictions, however, go beyond what was found experimentally so far, both qualitatively and quantitatively as discussed in Section 4. From a formal point of view (9) is equivalent to the original HKB equation (1) if the parameter a can take negative values. The derivation presented here has the advantage that it allows to discriminate between the two experimental manipulations (locations of the axes and coordination frequency), and gives the explicit form for the coupling term in the oscillator equations (8).

4. Predictions from the theory

We will proceed in two steps: First we discuss the qualitative features of the dynamical behavior we can expect if the axes locations are different from the extreme cases studied in the experiment, i.e., one axis above or below the hand, the other somewhere in between. Second, we will analyze the stability properties of the movement patterns quantitatively from the viewpoint of a stochastic theory.

4.1. Qualitative predictions

Different scenarios of what happens between the extreme cases $\sigma = 0$ and $\sigma = 1$ can be imagined. For instance, the exchange of stability between the fixed points $\phi_0 = 0$ and $\phi_\pi = \pi$ could occur as a shift of the potential landscape along the horizontal axis, i.e., the fixed points drift away from the former stable states as the symmetry parameter is varied. From the theoretical work above we conclude that this is not the case but make the following predictions in addition to the well-known properties of the original HKB system realized for $\sigma = 0$:

1. The fixed point locations under a change of the cycling frequency, k, or the symmetry parameter, σ, remains $\phi_0 = 0$ and $\phi_\pi = \pi$, i.e., the stable coordination patterns are either in-phase or anti-phase. Continuous dependencies of the locations of the points of stable relative phase along the ϕ-axis with these parameters should not exist.
2. There is a value of the symmetry parameter ($\sigma = 0.5$) where (if noise is present, as in all biological systems) the relative phase at high movement frequencies should undergo a random walk throughout the entire interval $[0, 2\pi]$, i.e., there is no preferred phase value. For slower movement frequencies the coordination pattern should switch randomly between the in-phase and anti-phase mode.
3. An initial anti-phase (in-phase) movement pattern should be more stable if the symmetry parameter is larger than zero (smaller than zero), i.e. the switching should take place at a higher cycling frequency compared to the extreme case $\sigma = 0$ ($\sigma = 1$). The critical value k_c, where the switching occurs, can be expressed as a function of σ by calculating the value of k for which the slope of the curves in the phase space plots vanishes at the intersection point with the horizontal axis, i.e., where the fixed point is neutrally stable. From (9), linearized around the fixed points (see below), we find

$$k_c = \begin{cases} -\frac{1}{4}(1 - 2\sigma) & \text{for } \phi_0 = 0, \\ \frac{1}{4}(1 - 2\sigma) & \text{for } \phi_\pi = \pi. \end{cases} \tag{11}$$

   As k has to be positive these values are valid for the fixed point ϕ_0 only if $\sigma > 1/2$ and for ϕ_π only if $\sigma < 1/2$.
4. Starting at a movement rate for which the system is monostable for $\sigma = 0$ ($\sigma = 1$), an increase (decrease) of the symmetry parameter will lead to a switch to the other coordination pattern at a certain value σ_c. If σ is now changed into the opposite direction the switch back to the initial

pattern will occur at a lower (higher) value than σ_c, i.e., the system shows hysteresis under a manipulation of the symmetry parameter. This can be seen best in Fig. 4 for $k = 0.15$. The in-phase mode is stable for small σ and becomes unstable at $\sigma_c = 0.8$ where the switch to anti-phase takes place. If σ is now decreased the switch back to in-phase will not occur until $\sigma = 0.2$ is reached.

All these predictions can be tested. Experiments are currently in preparation where the axis of rotation on one side is kept fixed above or below the hand while the location for the other hand can be varied systematically. When the axes are close together the setup corresponds to a small value of the symmetry parameter; a large parameter is realized when the axes are far apart.

4.2. Quantitative predictions

For quantitative predictions of the dependence of the movement patterns on the cycling frequency and the symmetry parameter σ it is necessary to know the relation between σ and the actual locations of the axes of rotation for both hands. For the extreme cases this relation is clear: for $\sigma = 0$ the axes are located on the same side of the hands whereas $\sigma = 1$ corresponds to axes on opposite sides. All values in between can be realized by keeping one axis fixed above or below and varying the location of the other. We will assume here that σ also vanishes if the vertical position of the axes for both hands is the same and that the symmetry parameter depends only on the relative positions of the two axes l_1, l_2 as shown in Fig. 1(b).

For the general case we expect σ to be a function of l_1 and l_2 like

$$\sigma = \left| \frac{l_1 - l_2}{L} \right| \quad \text{or, more general } \sigma = \left| \frac{l_1 - l_2}{L} \right|^{\epsilon}, \tag{12}$$

where L is the distance between the extreme cases, i.e., the length of the manipulandum. The value of $\sigma = 1/2$ is not necessarily realized for $|l_1 - l_2| = L/2$ what the exponent ϵ accounts for. In fact, the locations of the axes for this value may be different for the different conditions, i.e., for an initial pronation and supination movement, or whether the dominating hand is pronating or supinating, and has to be determined experimentally as discussed later.

4.3. The influence of noise

Human movements are not exactly reproducible and differ slightly from cycle to cycle or trial to trial. As a consequence during an experiment subjects cannot reproduce the exact same relative phase even for parameters where no switching takes place. In the original HKB system the dynamics of the relative phase around stable fixed points is therefore not a single constant value but a distribution function. The presence of stochastic fluctuations may also lead to switching from ϕ_π to ϕ_0 while both fixed points are still stable but the potential minimum at ϕ_π is shallow. The more shallow this minimum the earlier a switch will occur (on average over many trials) and this phenomenon is quantitatively described by the so-called mean first passage time (MFPT) (see Schöner, Haken, and Kelso, 1986).

Qualitatively new phenomena can be expected with the extension due to the symmetry parameter σ. Now there exist regions in parameter space where both minima of the potential function are shallow or the potential is entirely flat as seen in Fig. 4. For the former case we expect the relative phase to switch back and forth between the fixed points, for the latter ϕ will undergo a random walk. To capture these phenomena quantitatively and relate experimental data to the theory, a stochastic description is necessary. For readers unfamiliar with stochastic systems we give a brief introduction on the influence of noise on the dynamics in Appendix B.

4.4. Stability of the movement patterns from a stochastic theory

In the presence of noise a stochastic term has to be added to (9) which then becomes a Langevin equation of the form

$$\dot{\phi} = -(1-2\sigma)a\sin\phi - 2b\sin 2\phi + \sqrt{Q}\xi(t), \tag{13}$$

where $\xi(t)$ is uncorrelated (white) noise with zero mean and a Gaussian distribution

$$\langle\xi(t)\rangle = 0 \quad \text{and} \quad \langle\xi(t)\xi(t')\rangle = \delta(t-t'), \tag{14}$$

where Q is the amplitude of the stochastic force and $\langle\cdots\rangle$ represents the ensemble average across different realizations.

We distinguish three different situations corresponding to different regions in parameter space:

1. Two stable states exist which is the case for low cycling frequencies independent of the symmetry parameter.

2. Only a single stable state exists which is found for high cycling frequencies and the symmetry parameter either small (around zero) or large (around one).
3. States exist in the system which are stable in purely deterministic situations but the minima in the potential are shallow. If fluctuations are present they can include transitions into more stable states or lead to a kind of random walk for the relative phase. The former is predicted for medium movement rates and σ around zero and one. The latter should be found for high movement rates and σ around one half.

For the first two cases the movement patterns are stable either in-phase or anti-phase and transitions or drift of the relative phase do not happen within the time scale of observation. The stability of the fixed points depend on the cycling frequency and on the symmetry parameter, and is given quantitatively by the Jacobian of (13). Graphically this is expressed as the curvature at the extrema of the potential functions in Fig. 4. As the system stays in the vicinity of the fixed points we can use the local dynamical behavior and estimate the stability from the linearization of (13) around the fixed points ϕ_0 and ϕ_π. For the third case we will have to deal with the full system.

4.5. Local dynamics around the fixed points

It is straightforward to calculate the linearization of (13) from a Taylor expansion around the fixed points ϕ_0 and ϕ_π:

$$\dot{\phi} \approx \begin{cases} -\{(1-2\sigma)a + 4b\}\phi + \sqrt{Q}\xi(t) & \text{for } \phi_0 = 0, \\ \{(1-2\sigma)a - 4b\}(\phi - \pi) + \sqrt{Q}\xi(t) & \text{for } \phi_\pi = \pi. \end{cases} \tag{15}$$

The (15) represents two Ornstein–Uhlenbeck processes of the form

$$\dot{\phi} = -\gamma\phi + \sqrt{Q}\xi_t \tag{16}$$

whose stationary distribution $p(\phi) = p(\phi, t \to \infty)$ can be calculated as the stationary solution from the corresponding Fokker–Planck equation

$$\dot{p}(\phi, t) = \frac{\partial}{\partial\phi}\{\gamma\phi\ p(\phi, t)\} + \frac{Q}{2}\frac{\partial^2}{\partial\phi^2}p(\phi, t) = 0. \tag{17}$$

This (normalized) solution is a Gaussian distribution which reads

$$p(\phi) = N\,\mathrm{e}^{-(2/Q)V(\phi)} \quad \text{with } V(\phi) = \frac{\gamma}{2}\phi^2 \quad \text{and} \quad N = \sqrt{\frac{\gamma}{\pi Q}}. \tag{18}$$

By dropping t in the argument and introducing $\sqrt{\delta}$ as the standard deviation of the distribution or the variance in the times series we obtain

$$P(\phi) = N\,\mathrm{e}^{-(\gamma/Q)\phi^2} = \frac{1}{\sqrt{2\pi\delta}}\,\mathrm{e}^{-(1/2\delta)\phi^2}$$
$$\text{with } \delta = \int_{-\infty}^{\infty} \mathrm{d}\phi\; p(\phi)\;\phi^2 = \frac{1}{T}\int_0^T \mathrm{d}t\;\phi^2(t). \tag{19}$$

From (19), we find a relation between the experimentally accessible quantity δ and the parameters in the stochastic theory γ and Q, namely

$$\frac{\gamma}{Q} = \frac{1}{2\delta} \quad \text{or } \delta = \frac{Q}{2\gamma}. \tag{20}$$

We still need a second independent quantity from the experimental data to determine γ and Q uniquely. This can be found from the autocorrelation function $G(\tau)$ which falls off exponentially for the Ornstein–Uhlenbeck process (16) with a time constant of γ^{-1},

$$G(\tau) = \lim_{T\to\infty}\frac{1}{2T}\int_{-T}^{T}\mathrm{d}t\;\phi(t)\;\phi(t+\tau) = \frac{Q}{\gamma}\,\mathrm{e}^{-\gamma|\tau|}, \tag{21}$$

or even easier from the Fourier transform of $G(\tau)$ which is the spectrum of $\phi(t)$. From this relation (known as Wiener–Khinchin theorem) the analytic form of the spectrum can be calculated and turns out to be a Lorentzian which reads

$$S(\omega) = \mathscr{F}\{G(t)\} = |\mathscr{F}\{\phi(t)\}|^2 = \frac{Q}{\omega^2+\gamma^2}$$
$$\text{where } \mathscr{F}\{\cdots\} = \int_{-\infty}^{\infty}\cdots\,\mathrm{d}t\,\mathrm{e}^{-\mathrm{i}\omega t} \tag{22}$$

represents the Fourier transform. These functions have the property that at $\omega = \gamma$ they have fallen off to half of their value at $\omega = 0$. Fig. 5 shows how the values of δ and γ can be read off from the Gaussian distribution and the Lorentzian spectrum. With these two quantities the dynamical behavior of the system in the vicinity of stable fixed points with deep minima in the potential is completely characterized.

Here we have treated the relative phase as a quantity that can take values between $\pm\infty$ which allowed us to solve the Fokker–Planck equation (17), and calculate the autocorrelation function and the spectrum analytically. Of course, as a cyclic quantity ϕ is actually restricted to the interval $[0, 2\pi]$. This

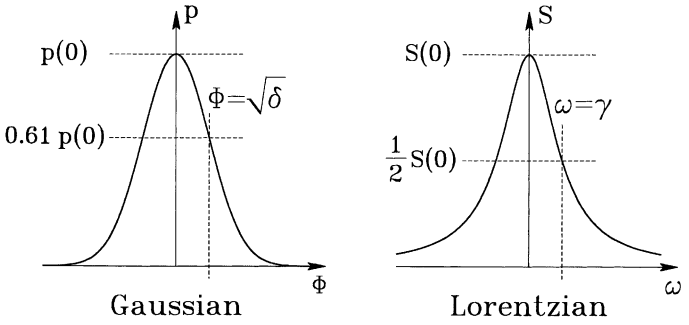

Fig. 5. Reading the values of δ and γ from a Gaussian distribution and a Lorentzian spectrum. For the standard deviation of the Gaussian the actual value is at $e^{-(1/2)}p(0)$.

procedure is justified because the probability distribution has to fall off fast in the vicinity of the fixed point for the linearization to be valid, i.e., $\delta \ll \pi$. Therefore, the contributions to the integrals from regions outside about $\pm\pi/2$ around the fixed points can be neglected.

4.6. Quantities from the nonlinear system

In regions in parameter space where the potential minima are shallow the linearization around the fixed point will not give a valid description of the dynamical properties because transitions into other states or random walk behavior of the relative phase will occur even if the movement frequency remains constant. In these situations the system is not confined to a small region of relative phase but explores the entire $[0, 2\pi]$ interval. For the random walk this is obvious but also for a descent into a deeper minimum on one trial the switch in relative phase may occur in one direction (say $\pi \to 0$), on another trial it may be in the other direction ($\pi \to 2\pi$) so that all values are reached at some point [2]. Histograms for different values of the symmetry parameter and movement frequency should look like the stationary distribution functions shown in Fig. 6 which are given by

$$p(\phi) = N\,e^{-(2/Q)V(\phi)} \quad \text{with } V(\phi) = -\cos\phi - k\cos 2\phi \tag{23}$$

with N a normalization constant.

[2] Here we assume the potential to be perfectly symmetric with respect to the $\phi = 0$ axis. Differences between pronation and supination may break this symmetry and lead to a preferred direction for the switching.

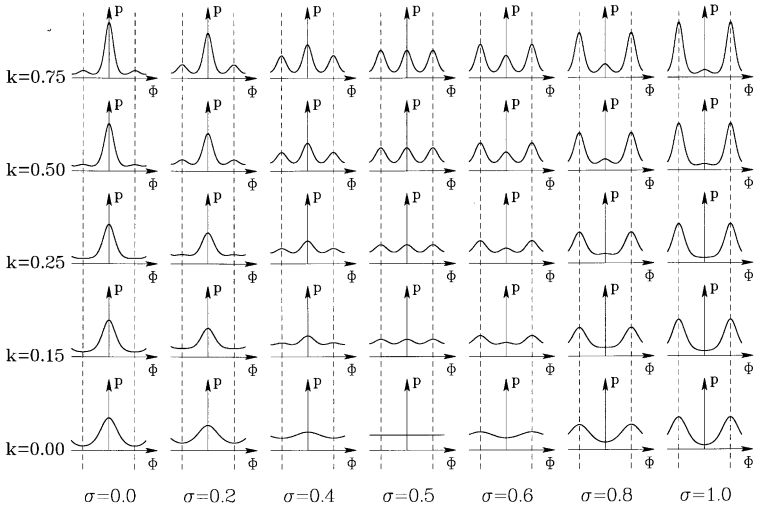

Fig. 6. The probability distribution for different values of σ and $k = b/a$. Vertical dashed lines correspond to $\phi = \pm\pi$.

These functions allow to identify the value of $\sigma = 0.5$ for the symmetry parameter as the distance between the axes of rotations $|l_1 - l_2|$, where the maxima at ϕ_0 and ϕ_π are the same (or where there are no extrema at all), in other words, where a symmetry exists along the vertical axis $\phi = \pi/2$. These stationary distributions can only be observed if the system is sufficiently unstable that it leaves the vicinity of its fixed point within the time of the experimental observation. The mean first passage time $T_{\pi\to 0}$ for a movement initially anti-phase to the in-phase state, i.e., a switch from ϕ_π to ϕ_0 is given by

$$T_{\pi\to 0} = \frac{2}{Q}\int_{\pi}^{0} \mathrm{d}\phi\, \mathrm{e}^{(2/Q)V(\phi)} \int_{\pi}^{\phi} \mathrm{d}\psi\, \mathrm{e}^{(2/Q)V(\psi)} \tag{24}$$

and is shown for different values of k and σ in Fig. 7. The circles indicate the values of k where the fixed point becomes unstable. Note that the mean first passage time increases rapidly when these values are passed.

The simplest case is $k = 0$ and $\sigma = 0.5$ for which the potential is entirely flat and the MFPT depends only on the noise strength Q:

$$T_{\pi\to 0} = \frac{\pi^2}{Q}. \tag{25}$$

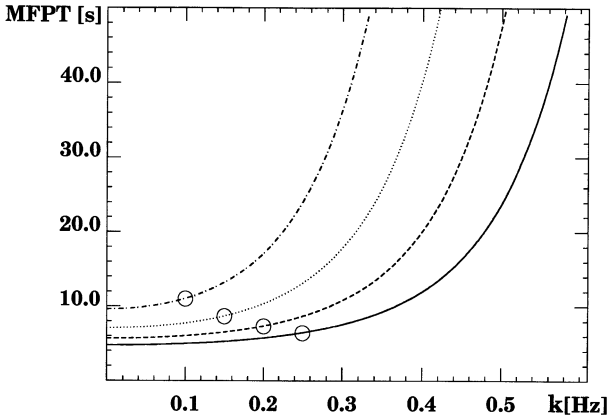

Fig. 7. The mean first passage time calculated from (24) as a function of k for different values of σ ($\sigma = 0, 0.1, 0.2, 0.3$), solid, dashed, dotted, dashed–dotted lines, respectively). The open circles indicate the values of k where the fixed point becomes unstable.

For the parameter $Q = 0.25$ used in Fig. 7 this leads to $T_{\pi\to 0} \approx 40$ s (a case not shown in Fig. 7).

5. Relating the quantities from theory and experiment

This section is devoted to the problem of how to determine the parameters that can be found experimentally and how to relate them to the quantities used in the theory. The general form of the HKB model derived here (13) contains four parameters a, b, σ and Q which have be to determined from the time series. Again, we distinguish between the regions in parameter space where the movement is stable in the vicinity of a fixed point and regions where transitions and drifts occur. We will restrict ourselves here to an explicit discussion of the former case and publish the latter elsewhere together with experimental data as soon as they are available. The first problem is to establish a relation between the symmetry parameter σ and the axes locations l_1 and l_2. As in Section 4.2 we assume that this relation is of the form

$$\sigma = \left| \frac{l_1 - l_2}{L} \right|^{\epsilon}. \tag{26}$$

This functional form is an operational assumption and cannot be derived from theoretical reasoning. However, assuming the validity of (26) we can

determine the parameter ϵ from the cases $\sigma = 1/2$. For the two cases above we have to find the values of $|l_1 - l_2|$, where the width δ of the distribution is the same for around the fixed points ϕ_0 and ϕ_π for the former and where the bimodal distribution functions are symmetric for the latter. For $\sigma = 1/2, \epsilon$ is given by

$$\epsilon = \frac{\ln 2}{\ln L - \ln|l_1 - l_2|}. \tag{27}$$

This value has to be determined for all movement frequencies for all of the four conditions.

If two stable states exist the parameters a, b and Q can be determined straightforwardly. From (15) and (20) we find

$$\begin{aligned} \delta_0 &= 2Q_0\{(1-2\sigma)a + 4b\}^{-1} \quad \text{for } \phi_0, \\ \delta_\pi &= -2Q_\pi\{(1-2\sigma)a - 4b\}^{-1} \quad \text{for } \phi_\pi, \end{aligned} \tag{28}$$

which can be readily solved for a and b:

$$\begin{aligned} a &= \frac{1}{1-2\sigma}\left\{\frac{Q_0}{\delta_0} - \frac{Q_\pi}{\delta_\pi}\right\}, \\ b &= \frac{1}{4}\left\{\frac{Q_0}{\delta_0} + \frac{Q_\pi}{\delta_\pi}\right\}. \end{aligned} \tag{29}$$

The noise strengths Q_0 and Q_π are determined from (20) and are given by

$$Q_0 = 2\delta_0\gamma_0 \quad \text{and} \quad Q_\pi = 2\delta_\pi\gamma_\pi, \text{ respectively.} \tag{30}$$

If only one stable state exists we cannot determine all three parameters but only k and Q as

$$k = \frac{Q}{2\delta} \quad \text{and} \quad Q = 2\delta\gamma. \tag{31}$$

To find the parameters in the cases where transitions and drifts of the relative phase exist is much more difficult and computationally intensive. We have to deal with the fully nonlinear system which is described by the stationary distribution

$$\begin{aligned} p_s(\phi) &= N\,\mathrm{e}^{(2/Q)(a\cos\phi + b\cos 2\phi)} \\ &\text{with } N = \left\{\int_{-\pi}^{\pi} \mathrm{d}\phi\,\mathrm{e}^{(2/Q)(a\cos\phi + b\cos 2\phi)}\right\}^{-1}. \end{aligned} \tag{32}$$

However, there are two procedures that allow to calculate the drift and diffusion terms in the Fokker–Plank equation (17), i.e., $K(q)$ and Q, respectively. The first procedure was proposed by Haken (1988) and further elaborated by Borland and Haken (1992a,b), the second was first applied to turbulent flow by Friedrich and Peinke (1997) and described in a more general form in Siegert, Friedrich and Peinke (1998). Both of them work for simulated time series but it needs to be determined which one is better for dealing with the experimental data in question.

6. Summary and conclusion

We presented predictions about coordinated human movement behavior under a manipulation of a symmetry parameter σ which controls the stability of the different coordination states, i.e. in-phase and anti-phase. The breaking of symmetry is generally achieved through environmental and/or intrinsic constraints. Particularly, in the Carson et al. experiment, the symmetry parameter σ is given by the position of the axes of rotation and can be manipulated in a continuous fashion. As the theoretical analysis shows, we expect new phenomena to be observed experimentally that so far (to our knowledge) have not been found like symmetric phase drifts [3] or back and forth switches between the fixed points ϕ_0 and ϕ_π. The theory also predicts that these fixed points are not shifted (as in the case with broken symmetry due to different eigenfrequencies of the components). Finally, the procedures outlined in the previous section allow to determine the theoretical parameters as a function of the cycling frequency and the symmetry parameter, with an independent consistency check by calculating the mean first passage time and its comparison with experimentally measured values.

Acknowledgements

Research supported by NIMH (Neuroscience Research Branch) Grant MH42900. This work originated during a workshop at Penn State organized

[3] Phase wandering in one direction is a known phenomenon that has been predicted and observed in systems where the symmetry is broken as in coordinated movement between an arm and a leg (Kelso and Jeka, 1992) or in the perception-action paradigm (Kelso et al., 1990) which also show a shift of the fixed point.

by Dagmar Sternad with financial support from the Santa Fe Institute. We thank Richard Carson for fruitful discussions and for sharing the data shown in Fig. 2.

Appendix A. The extended HKB equation

In order to derive an equation for the dynamics of relative phase we rewrite the quantities x_k in the way

$$x_k = r\,\mathrm{e}^{\mathrm{i}\varphi_k}\,\mathrm{e}^{\mathrm{i}\omega t} + \text{c.c.} \quad \text{and} \quad \dot{x}_k = \mathrm{i}\omega r\,\mathrm{e}^{\mathrm{i}\varphi_k}\,\mathrm{e}^{\mathrm{i}\omega t} + \text{c.c.} \tag{A.1}$$

Here we have used two standard approximations, the rotating wave approximation by assuming that the dominating frequency in the system is ω and the slowly varying amplitude approximation, i.e., the time dependence of the phases $\varphi_k(t)$ is slow compared to the time scale given by $T = 2\pi/\omega$ and therefore, the derivatives $\dot{\varphi}_k \ll \omega$ can be neglected.

With (A.1) we rewrite the nonlinearities that appear in the new coupling terms in (8):

$$\begin{aligned}
\dot{x}_2 x_1^2 &= \mathrm{i}\omega r^3\left(\mathrm{e}^{\mathrm{i}\varphi_2}\,\mathrm{e}^{\mathrm{i}\omega t} - \mathrm{e}^{-\mathrm{i}\phi_2}\,\mathrm{e}^{-\mathrm{i}\omega t}\right)\left(\mathrm{e}^{2\mathrm{i}\varphi_1}\,\mathrm{e}^{2\mathrm{i}\omega t} + \mathrm{e}^{-2\mathrm{i}\varphi_1}\,\mathrm{e}^{-2\mathrm{i}\omega t} + 2\right) + \text{c.c.} \\
&= \mathrm{i}\omega r^3\left(2\mathrm{e}^{\mathrm{i}\varphi_2} - \mathrm{e}^{\mathrm{i}(2\varphi_1-\varphi_2)}\right)\mathrm{e}^{\mathrm{i}\omega t} + \text{c.c.}, \\
\dot{x}_2 x_2^2 &= \mathrm{i}\omega r^3\left(\mathrm{e}^{\mathrm{i}\varphi_2}\,\mathrm{e}^{\mathrm{i}\omega t} - \mathrm{e}^{-\mathrm{i}\phi_2}\,\mathrm{e}^{-\mathrm{i}\omega t}\right)\left(\mathrm{e}^{2\mathrm{i}\varphi_2}\,\mathrm{e}^{2\mathrm{i}\omega t} + \mathrm{e}^{-2\mathrm{i}\varphi_2}\,\mathrm{e}^{-2\mathrm{i}\omega t} + 2\right) + \text{c.c.} \\
&= \mathrm{i}\omega r^3\left(2\mathrm{e}^{\mathrm{i}\varphi_2} - \mathrm{e}^{\mathrm{i}\varphi_2}\right)\mathrm{e}^{\mathrm{i}\omega t} + \text{c.c.} = \mathrm{i}\omega r^3\mathrm{e}^{\mathrm{i}\varphi_2}\,\mathrm{e}^{\mathrm{i}\omega t} + \text{c.c.}, \\
\dot{x}_1 x_1 x_2 &= \mathrm{i}\omega r^3\left(\mathrm{e}^{\mathrm{i}\varphi_1}\,\mathrm{e}^{\mathrm{i}\omega t} - \mathrm{e}^{-\mathrm{i}\phi_2}\,\mathrm{e}^{-\mathrm{i}\omega t}\right)\left(\mathrm{e}^{\mathrm{i}\varphi_1}\,\mathrm{e}^{\mathrm{i}\omega t} + \mathrm{e}^{-\mathrm{i}\phi_1}\,\mathrm{e}^{-\mathrm{i}\omega t}\right)\left(\mathrm{e}^{\mathrm{i}\varphi_2}\,\mathrm{e}^{\mathrm{i}\omega t} + \mathrm{e}^{-\mathrm{i}\phi_2}\,\mathrm{e}^{-\mathrm{i}\omega t}\right) + \text{c.c.} \\
&= \mathrm{i}\omega r^3\,\mathrm{e}^{\mathrm{i}(2\varphi_1-\varphi_2)}\,\mathrm{e}^{\mathrm{i}\omega t} + \text{c.c.}
\end{aligned} \tag{A.2}$$

Inserting (A.2) into (8) we obtain

$$\begin{aligned}
\dot{\varphi}_1 + \cdots &= \cdots + 2\sigma\left\{\mathrm{i}\alpha\mathrm{e}^{-\mathrm{i}\varphi_1} + \mathrm{i}\beta r^2\left[2\mathrm{e}^{-\mathrm{i}(\varphi_1-\varphi_2)} - \mathrm{e}^{\mathrm{i}(\varphi_1-\varphi_2)} + \mathrm{e}^{\mathrm{i}(\varphi_1-\varphi_2)} + 2\mathrm{e}^{\mathrm{i}(\varphi_1-\varphi_2)}\right]\right\} \\
&= \cdots + 2\sigma\mathrm{i}\left\{\alpha + \beta r^2\left[3\mathrm{e}^{-\mathrm{i}\phi} + \mathrm{e}^{\mathrm{i}\phi}\right]\right\} = \cdots + 2\sigma\mathrm{i}\left\{\alpha + 2\beta r^2\left[\mathrm{e}^{-\mathrm{i}\phi} + \cos\phi\right]\right\}, \\
\dot{\varphi}_2 + \cdots &= \cdots + 2\sigma\mathrm{i}\left\{\alpha + 2\beta r^2\left[\mathrm{e}^{-\mathrm{i}\phi} + \cos\phi\right]\right\},
\end{aligned} \tag{A.3}$$

where $\cdots$ on the right-hand side represents the contributions from the original HKB coupling. For the relative phase $\phi = \varphi_1 - \varphi_2$ we find

$$\dot{\phi} = (1 - 2\sigma)(\alpha + 2\beta r^2)\sin\phi - \beta r^2 \sin 2\phi \tag{A.4}$$

and with the common abbreviations $\alpha + 2\beta r^2 = -a$ and $\beta r^2 = 2b$ we obtain the extended dynamics of the relative phase in its final form:

$$\dot{\phi} = -(1 - 2\sigma)a\sin\phi - 2b\sin 2\phi. \tag{A.5}$$

Appendix B. The stochastic description of dynamical systems

Systems with random noise are described by introducing a stochastic term into the equation of motion. There are several ways this can be done but we will restrict ourselves to the easiest case which is additive uncorrelated (white) noise with a Gaussian distribution. Here we give a brief summary of the properties of such systems and refer the reader to standard textbooks on stochastic systems (e.g. Haken, 1977; Gardiner, 1983; Risken, 1984; see also Schöner et al., 1986) for details,

A one-dimensional stochastic system for a variable q is described by an equation of motion, called a Langevin equation, of the form

$$\dot{q} = K(q) + \sqrt{Q}\xi(t), \tag{B.1}$$

where $K(q)$ is a deterministic force term, Q represents the noise strength and $\xi(t)$ is a stochastic force consisting of uncorrelated (white) noise with a zero mean and a Gaussian distribution. The former two properties are formally expressed as

$$\langle \xi(t) \rangle = 0 \quad \text{and} \quad \langle \xi(t)\xi(t') \rangle = \delta(t - t') \tag{B.2}$$

where $\langle \cdots \rangle$ represents the ensemble mean over different realizations. If we assume the deterministic force in (B.1) to be linear, $K(q) = -\gamma q$, a formal solution $q(t)$ can be obtained:

$$q(t) = q(t = 0)\, \mathrm{e}^{-\gamma(t)} + \sqrt{Q} \int_0^t \mathrm{d}t'\ \xi(t')\, \mathrm{e}^{-\alpha(t-t')}. \tag{B.3}$$

Due to the explicit dependence on $\xi(t')$ this solution is different for each realization and, unfortunately, cannot be compared with the experimental data because we do not know $\xi(t')$ for the particular realizations. The statistical properties of q, expressed by the distribution $p(q,t)$ for an ensemble average, are independent of the explicit form of $\xi(t')$ as long as (B.2) is fulfilled. The function $p(q,t)$ represents the probability density and $p(q,t)\,\mathrm{d}q$ is the probability for finding the system in the interval $[q, q + \mathrm{d}q]$ at time t. This distribution can be calculated from the Fokker–Planck equation that corresponds to the Langevin equation (B.1) and reads

$$\dot{p}(q,t) = -\frac{\partial}{\partial q}\{K(q)\, p(q,t)\} + \frac{Q}{2}\frac{\partial^2}{\partial q^2}\, p(q,t). \tag{B.4}$$

The first term on the right-hand side of (B.4) carries the deterministic part of the Langevin equation and is called the drift coefficient whereas the second contains the noise and is know as diffusion coefficient.

For the so-called natural boundary conditions, i.e.,

$$p(q \to \pm\infty, t) = \frac{\partial}{\partial q} p(q \to \pm\infty, t) = 0, \tag{B.5}$$

the stationary solution $p(q)$ of the partial differential equation (B.4) can be readily calculated:

$$p(q) = p(q, t \to \infty) = N\,\mathrm{e}^{-(2/Q)V(q)} \quad \text{with } K(q) = -\frac{\partial}{\partial q} V(q), \tag{B.6}$$

where $V(q)$ is the potential corresponding to the deterministic force $K(q)$ in (B.1). The constant N normalizes the distribution and can be expressed formally as

$$N = \left\{ \int_{-\infty}^{\infty} \mathrm{e}^{-(2/Q)V(q)} \right\}^{-1} \quad \text{to ensure } \int_{-\infty}^{\infty} p(q)\,\mathrm{d}q = 1. \tag{B.7}$$

The relation between a potential $V(q)$ and the corresponding stationary distribution $p(q)$ is shown in Fig. 8 (top). Obviously, the probability to find the system is high where the potential is low and vice versa.

Beside the distribution a second important quantity to describe stochastic systems is the time it takes (on average) to reach a point $q = b$ if it was initially located at $q = a$. This question is in particular interesting for a situation as in Fig. 8 (top) where a is at the bottom of a shallow minimum and b is a deep minimum of the potential. In a deterministic system with no stochastic forces present a is a stable fixed point and if we chose a as an initial condition it will stay there forever. In the stochastic case with fluctuations there is a finite probability that the system gets kicked over the hill at c and reaches the deeper minimum b. The time it takes on average to reach b when it was initially located at a is called the mean first passage time (MFPT) $T_{a\to b}$. It can be shown (Gardiner, 1983) that this time is given by

$$T_{a\to b} = \frac{2}{Q} \int_a^b \mathrm{d}y\, \mathrm{e}^{(2/Q)V(y)} \int_a^y \mathrm{d}x\, \mathrm{e}^{-(2/Q)V(x)}, \tag{B.8}$$

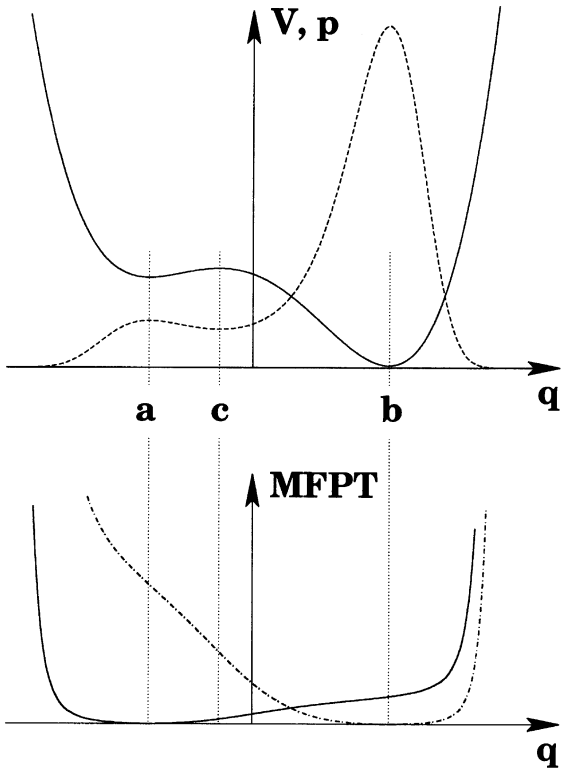

Fig. 8. Top: A potential function (solid) and the corresponding stationary probability distribution (dashed). Bottom: The mean first passage time (MFPT) for the system to reach a location q when initially at a (solid) or at b (dashed–doted).

which can be generalized to the question how long it takes the system on average to reach a point q when it was located initially at a or b. These times are $T_{a\to q}$ and $T_{b\to q}$, respectively,

$$T_{a\to q} = \frac{2}{Q}\int_a^q \mathrm{d}y\, \mathrm{e}^{(2/Q)V(y)} \int_a^y \mathrm{d}x\, \mathrm{e}^{-(2/Q)V(x)},$$
$$T_{b\to q} = \frac{2}{Q}\int_b^q \mathrm{d}y\, \mathrm{e}^{(2/Q)V(y)} \int_b^y \mathrm{d}x\, \mathrm{e}^{-(2/Q)V(x)}. \tag{B.9}$$

Plots for both of these times are shown in Fig. 8 (bottom). Evidently, the system can also be kicked into the shallow minimum at a when it was initially

at b but it takes much longer. For the potential used in Fig. 8 we find $T_{a\to b} = 1.1$ and $T_{b\to a} = 5.6$ (in arbitrary units).

References

Borland, L., & Haken, H. (1992a). Unbiased determination of forces causing observed processes. The case of additive and weak multiplicative noise. *Zeitschrift für Physik B*, *81*, 95–103.

Borland, L., & Haken, H. (1992b). Unbiased estimate of forces from measured correlation functions, including the case of strong multiplicative noise. *Annales de Physique*, *1*, 452–459.

Carson, R. G., Rick, S., Smethurst, C. J., Lison, J. F., & Byblow, W. D. (2000). Neuromuscular-skeletal constraints upon the dynamics of unimanual and bimanual coordination. *Experimental Brain Research*, *131*, 196–214.

Friedrich, R., & Peinke, J. (1997). Statistical properties of a turbulent cascade. *Physica D*, *102*, 147–155.

Gardiner, C. W. (1983). *Handbook of stochastic methods for physics, chemistry, and the natural sciences* (2nd ed.). Berlin: Springer.

Haken, H. (1977). *Synergetics: An introduction* (3rd ed.). Berlin: Springer.

Haken, H. (1988). *Information and selforganization. A macroscopic approach to complex systems*. Berlin: Springer.

Haken, H., Kelso, J. A. S., & Bunz, H. (1985). A theoretical model of phase transitions in human movements. *Biological Cybernetics*, *51*, 347–356.

Jirsa, V. K., Kelso, J. A. S., & Fuchs, A. (1998). Connecting coordination and behavioral dynamics: bimanual coordination. *Neural Computation*, *10*, 2019–2045.

Jirsa, V. K., Kelso, J. A. S., & Fuchs, A. (1999). Traversing scales of brain and behavioral organization III: Theoretical modeling. In C. Uhl (Ed.), *Analysis of neurophysiological brain functioning* (pp. 107–125). Berlin: Springer.

Kay, B. A., Kelso, J. A. S., Saltzman, E. L., & Schöner, G. (1987). Space-time behavior of single and bimanual rhythmical movements: Data and limit cycle model. *Journal of Experimental Psychology: Human Performance and Perception*, *13*, 178–192.

Kelso, J. A. S. (1984). Phase transitions and critical behavior in human bimanual coordination. *American Journal of Physiology*, *15*, 1000–1004.

Kelso, J. A. S., DelColle, J. D., & Schöner, G. (1990). Action-perception as a pattern forming process. In M. Jeannerod (Ed.), *Attention and Performance XIII* (pp. 139–169). Hillsdale, NJ: Erlbaum.

Kelso, J. A. S., & Jeka, J. J. (1992). Symmetry-breaking dynamics of human limb coordination. *Journal of Experimental Psychology: Human Perception and Performance*, *18*, 645–668.

Risken, H. (1984). *The Fokker–Planck equation: Methods of solutions and applications* (2nd ed.). Berlin: Springer.

Schmidt, R. C., Carello, C., & Turvey, M. T. (1990). Phase transitions and critical fluctuations in the visual coordination of rhythmic movements between people. *Journal of Experimental Psychology: Human Perception and Performance*, *16*, 247–277.

Schöner, G., Haken, H., & Kelso, J. A. S. (1986). A stochastic theory of phase transitions in human hand movements. *Biological Cybernetics*, *53*, 247–257.

Siegert, S., Friedrich, R., & Peinke, J. (1998). Analysis of data of stochastic systems. *Physics Letters A*, *243*, 275–280.